Doxorubicin Removal from Water using Acid-treated Activated Carbon, Multi-walled Carbon Nanotubes, and Montmorillonite

N. Rezaei, J. R. Shahrouzi,* A. Ebadi, F. Towfighi, and F. Moradi
Faculty of Chemical Engineering, Sahand University of Technology, Sahand New Town, Tabriz, Iran

doi: https://doi.org/10.15255/CABEQ.2023.2257
Original scientific paper
Received: September 2, 2023
Accepted: March 11, 2024

Medical wastewater is a significant contributor to environmental pollution, posing severe risks to both human health and the environment. To resolve this challenge, the removal of anti-cancer drugs from medical wastewater has been considered. This study investigated the removal of doxorubicin, an effective anti-cancer drug, from an aqueous solution using three types of adsorbents: activated carbon, multi-walled carbon nanotube, and montmorillonite. Our findings revealed that carbon nanotubes exhibited superior performance in doxorubicin removal from water compared to the other two adsorbents. Specifically, the maximum adsorption capacity of doxorubicin with an initial concentration of 50 mg L^{-1} on the carbon nanotube reached 500 mg g^{-1}. In addition, surface modification of the adsorbents with acid resulted in a 15 % and 41 % increase in adsorption capacity, and an 85 % and 67 % reduction in equilibrium time for carbon nanotube and montmorillonite, respectively. The increasing pH proved to enhance the adsorption efficiency of carbon nanotubes and activated carbon, with the best performance achieved at solution pH of 10 and 8 for MWCNTs and AC, respectively.

Keywords
activated carbon, adsorption, carbon nanotube, doxorubicin, montmorillonite

Introduction

Currently, cancer is one of the leading causes of death worldwide, with projected mortalities reaching 11.4 million by 2030[1]. Consequently, anti-cancer drugs are widely used due to their growing demand[2]. Doxorubicin (DOX) is one of the first clinical anthracyclines commonly used in cancer chemotherapy to treat several types of cancer, including solid tumors and hematological malignancies[3,4].

While anti-cancer drugs constitute a lower proportion of wastewater contaminants than other drugs, they have a more significant effect on human health and the environment[5]. Reports indicate that anti-cancer agents pose serious health risks, including carcinogenesis, genetic mutation, and adverse effects on fetal development[6]. Therefore, the removal of anti-cancer drugs from hospital wastewater is crucial for mitigating environmental hazards[7].

Various methods, such as biological methods, filtration, ozonation, chemical oxidation, advanced oxidation, and adsorption have been investigated for sewage treatment[8]. However, these techniques often suffer from drawbacks such as high energy consumption, limited removal capacities, high cost, and complicated operation[9]. Among the possible wastewater treatment techniques, the solid adsorbent adsorption process has shown great potential as a practical process[10,11]. The adsorption process offers various advantages, including exceptional efficiency, straightforward operation, simple design, a wide range of available adsorbents, and the ability to remove diverse contaminants, such as dyes[12,13], heavy metals[14], and antibiotics[15]. However, like all separation techniques, adsorption processes have limitations, including the high cost of some adsorbents, rapid saturation, and expensive regeneration, which must be considered[16]. Consequently, searching for regenerable, effective, and inexpensive adsorption materials remains a critical and ongoing task. Hence, the adsorption of drugs from wastewater has emerged as a key area of focus in recent research. The most remarkable aspect of these studies was the identification of effective and economical adsorbents. Recent studies have highlighted the effectiveness of various adsorbents, including activated carbon (AC)[17,18], nano clays like montmorillonite[19], and organobentonite[20], and carbon nanotubes (CNTs)[7] in pharmaceutical wastewater treatment.

Activated carbon, known for its enormous surface area, high porosity, and high adsorption capac-

*Corresponding author e-mail: shahrouzi@sut.ac.ir

ity, has been widely used in wastewater treatment. In general, the four main functional groups, such as carboxyl, carbonyl, phenols, and lactones in the AC structure, play a critical role in the adsorption of pollutants[21]. In addition, reports indicate that acid treatment of AC can increase the functional groups of AC and enhance its adsorption performance[22]. Carbon nanotubes (CNTs) can be described as one-dimensional layers of graphite, which are classified as single-walled nanotubes (SWNTs), double-walled nanotubes (DWNTs), and multi-walled nanotubes (MWNTs)[23]. CNTs have exceptional mechanical properties, such as high thermal and chemical stability, and large surface area[24]. These specific features make CNTs an excellent adsorbent for different purposes, such as for the removal of contaminants from wastewater[25], as nano-carriers[26], and for biomedical applications[27]. In addition, in surface-modified CNTs, the presence of oxygen-containing carboxyl and hydroxyl groups enhances their adsorption performance and adsorption capacity[28]. Additionally, clay minerals are inexpensive and abundant materials commonly used in various applications, such as in biomedicine, as biosensors, and in cosmetics[29]. Bentonite is a mineral clay primarily composed of montmorillonite[30]. Montmorillonite has been studied for decades, owing to its structural features, such as high surface area and cation exchange capacity, which render it suitable for pharmaceutical applications, as elucidated by Jayrajsinh[31]. Sodium montmorillonite (NaMMT) is a silica-alumina mineral composed of an octagonal alumina layer and two quartz-silica layers[32]. Moreover, by acid treatment of clay, certain mineral impurities are removed by exchangeable cations, such as H^+ and Al^{3+}, and a proton was replaced, increasing the surface area and acidity. The type of acid, process temperature, processing time, clay and non-clay minerals, chemical composition, type of cations between the layers, and other environmental factors affect the changes in surface area and microporous structure in acid-treated clays[33]. In contrast to the adsorption of commonly used drugs like antibiotics, the adsorption of anticancer drugs like methotrexate[10], ellipticine[34], epirubicin[35], cyclophosphamide, ifosfamide, and 5-fluorouracil has recently been considered[36]. In this sense, there have been notable efforts to investigate the adsorption of doxorubicin (DOX) onto different adsorbents, such as graphene oxide, carbon nanotubes[37], and silica[38], as documented in the literature. To highlight the primary novelty of this paper, according to references, it is noteworthy to emphasize the absence of reports regarding the adsorption of DOX by montmorillonite nano clay, despite its demonstrated potential for pharmaceuticals adsorption and common use in drug delivery. On the other hand, a literature gap exists concerning comparison of different adsorbents for DOX removal studies. Given the increased use of DOX in cancer therapy and the emerging challenge of hospital wastewater management, this study represents a step forward in investigating the efficacy of three conventional, cost-effective, and readily available adsorbents AC, CNTs, and NaMMT in removing DOX from aqueous solutions. Furthermore, the effect of acid treatment on the performance of these adsorbents, along with the influence of solution pH on adsorption capacity, was examined.

Materials and methods

Materials

DOX hydrochloride from Pfizer Co. (USA) served as the drug contaminant. AC was obtained from Scharlau Co. (Spain), possessing a surface area of 980 $m^2\ g^{-1}$ as utilized in this study. Multi-walled carbon nanotubes (MWCNTs) was purchased from Neutron Co. (Iran) with a specific surface area of 200 $m^2\ g^{-1}$, an average diameter from 10–20 nm, an average length of 30 μm, and a purity level of 95 %. Additionally, nano-sodium montmorillonite was supplied by Sigma-Aldrich Co. (USA) possessing a specific surface area of 250 $m^2\ g^{-1}$. Nitric acid (purity 63 %), hydrochloric acid (purity 37 %), and sodium hydroxide (purity 65 %) were purchased from Merck Co. (Germany). Deionized water was utilized throughout all experiments.

Acid-treatment

Acid treatment was employed to modify the surface of the adsorbents. To achieve this, 0.5 g of AC, 0.1 g of MWCNT, and 10 g of NaMMT were weighted with a precision of ±0.1 mg (Mettler Toledo-AE240, Switzerland), and then added to 50, 10, and 100 mL nitric acid 63 %, respectively. The resulting mixture was stirred for one hour at 80 °C and 500 rpm, then kept for 24 h at ambient temperature. The adsorbents were then washed with deionized water several times until the solution pH reached the same level as the deionized water. Finally, the adsorbent particles were filtered and dried in an oven at 80 °C for 18 h[20].

FTIR analysis

The performance of adsorbent materials in adsorption processes is highly dependent on their structural characteristics, including the number and nature of surface functional groups and surface porosity[39]. A crucial step in our research was FTIR analysis (Bruker, Tensor 27, Germany). This powerful analytical technique enabled us to identify the functional groups of pure and surface-modified adsorbents induced by the acid treatment.

Doxorubicin concentration determination

To initiate the experiment, we filled a cell with two mL of the doxorubicin solution and placed it in the spectrophotometer to determine the wavelength with maximum absorption. The absorption spectrum of the doxorubicin solution revealed a peak absorption at 481 nm. To ensure the utmost precision in determining the unknown concentration via UV analysis, a calibration curve was meticulously plotted. This curve was generated by adding solutions of varying concentrations, all below 50 ppm, and measuring their absorption at the peak wavelength of 481 nm. Upon completion of the measurements and calibration curve generation, a conversion factor of 0.0193 was derived to translate absorbance readings into concentrations.

pH measurement

To investigate how pH influences the removal of doxorubicin from water, solutions with a concentration of 50 mg L^{-1} and an initial pH of 5.6 were prepared. The pH was adjusted from 5 to 9 using trace amounts of hydrochloric acid and sodium hydroxide. Next, 5 mg of activated carbon adsorbent and 1 mg of carbon nanotube were added to 20 mL of these solutions, with pH values ranging from 5 to 9. These mixtures were then subjected to magnetic stirring. After reaching equilibrium in the kinetics phase, the samples were withdrawn and centrifuged for 25 minutes at 4000 rpm, after which the concentration of the remaining pharmaceutical pollutant was measured.

Adsorption kinetics experiments

For the kinetic study, 20 mL of DOX solution with an initial concentration of 50 mg L^{-1} and pH = 6.5, at 25 °C in a 50 mL beaker under constant stirring of 500 rpm, was mixed with 1, 5, and 10 mg of MWCNT, AC, and NaMMT, respectively. After 5 min, the sample was centrifuged at 3500 rpm for 25 min, following which the drug concentration in the sample solution was determined using a UV-vis spectrophotometer (UV-vis Jenway-6705, UK). This procedure was repeated at intervals of 10, 15, 25, 40, 60, 100, 150, 200, 250, and 300 minutes until adsorption equilibrium was attained.

The adsorption rate is a criterion for defining adsorbent performance[3]. Kinetics is an essential parameter in characterizing the adsorption dynamics of the adsorbate and can provide valuable insights into potential adsorption mechanisms, including diffusion and chemical reactions[7]. Two kinetic models were applied to fit the experimental adsorption data. Linearized Eqs. (1 and 2) express the pseudo-first-order and pseudo-second-order kinetic models, respectively:

$$\ln(q_e - q_t) = \ln(q_e) - k_1 t \quad (1)$$

$$\frac{t}{q_t} = \frac{1}{k_2 q_{e2}^2} + \frac{1}{q_{e2}} t \quad (2)$$

where q_e (mg g^{-1}) and q_t (mg g^{-1}) are the adsorption capacities of DOX at equilibrium time and time t (min), respectively, k_1 (min^{-1}) is the equilibrium rate constant of pseudo-first sorption, k_2 (g mg^{-1} min^{-1}) is the pseudo-second-order rate constant[40]. The pseudo-first-order kinetic model suggests that adsorption occurs via physisorption and is simply reversible, whereas the pseudo-second-order model suggests that adsorption occurs through chemisorption[14]. The amount of adsorbed DOX on adsorbents was calculated using Eq. (3)[8].

$$q_e - q_0 = \frac{(C_0 - C_e)V}{m} \quad (3)$$

where q_0 (mg g^{-1}) is the initially adsorbed amount of DOX; C_0 (mg L^{-1}) and C_e (mg L^{-1}) are the initial and equilibrium concentrations in the liquid phase, respectively; V (mL) is volume, and m (mg) is adsorbent mass.

Adsorption isotherm experiments

The adsorption isotherm investigates the relationship between equilibrium adsorption capacity and equilibrium concentration at the same temperature. To determine the adsorption isotherms, 20 mL of solutions with different initial concentrations of 25, 30, 35, 40, 45, and 50 mg L^{-1} in 1, 5, and 10 mg of MWCNTS, AC, and NaMMT, respectively, were stirred until equilibrium was attained. The samples were then centrifuged at 3500 rpm for 25 min, and the residual concentration of the drug was measured. It is worth noting that the amount of adsorbents utilized in this study was chosen based on their difference in adsorption capacities; however, the comparison was ultimately made based on the adsorption capacity, which is independent of the adsorbent quantity. Two popular models were employed to analyze the adsorption isotherm, namely the Langmuir and Freundlich models. The Langmuir isotherm assumes monolayer adsorption, homogeneous adsorbent surface, and uniform energy across all active sites. The linearized isotherm is as follows (Eq. 4):

$$\frac{C_e}{q_e} = \frac{1}{q_m b_l} + \frac{C_e}{q_m} \quad (4)$$

where q_m (mg g^{-1}) is the maximum adsorption capacity, and b_l (L mg^{-1}) is the adsorption equilibrium constant related to the energy of adsorption. The Freundlich isotherm, as an empirical model, is particularly suitable for systems with decent concentrations (in the mg L^{-1} range). The linearized isotherm model can be written as Eq. (5).

$$\ln(q_e) = \frac{1}{n_F}\ln(C_e) + \ln(k_F) \quad (5)$$

where k_F is the Freundlich constant related to adsorption capacity at an equilibrium concentration of 1 μg mL^{-1} and adsorption intensity of the adsorbent, and n is the adsorption intensity[20].

Results and discussion

FTIR analysis

As depicted in Fig. 1, FTIR analysis reveals significant transformations in MWCNTs following acid treatment. A notable change is the emergence of the C=O stretching band at 1700 cm^{-1} and the increase in the O–H band at 3500 cm^{-1}, both attributed to the formation of carbonyl groups due to acid oxidation[41]. Regarding the functionalization process of MWCNTs, the acid activation method with a strong acid was utilized. This method induced the generation of carboxyl and hydroxyl groups on the CNT surface through the oxidation of double bonds on the graphene walls, thereby enhancing the adsorption capacity of CNT[35]. DOX contains O–H and amino groups, which have the potential to form interactions with oxidized carbon nanotubes. The hydrogen bonding between the oxygen-containing groups in the adsorbent and the O–H group of DOX is considered one of the possible mechanisms to describe the effect of the O–H substitution on the adsorption of organic compounds by CNT. Theoretically, four types of adsorption sites, including the external surface, internal porosity, groove region, and interstitial pores, are available for adsorption onto CNT. Pan *et al.* reported that the outer and groove regions are more accessible than the internal and interstitial pores for adsorption, and that the blocked internal porosities are opened by activation with nitric acid. Therefore, since the DOX molecular structure is relatively larger, the outer surface is much more available for the adsorption of this molecule than the interstitials. In other words, the external surface area is the critical parameter in adsorption. The higher adsorption of DOX on treated CNT compared to primary CNT can be attributed to the difference in the accessibility of adsorbent sites[41].

Moreover, Fig. 1(b) presents the key findings of FTIR analysis for AC before and after acid treatment. The peak at the wavenumber of 3500 cm^{-1} indicates phenolic type O–H bands, and the stretching band at 2887 cm^{-1} is attributed to the existence of C–H bonds. Nitrogenous carbonyl groups (amides) and carboxyl can be detected at 1700 and 1112 cm^{-1} wavenumbers, respectively. The results reveal that acid activation had slightly increased the –OH and N–COOH functional groups[42].

Additionally, the FTIR analysis of NaMMT is presented in Fig. 1(c). The peaks in wavenumbers 1033 and 912 cm^{-1} indicate the Si–O and Al–O bands, respectively. The peaks in the wavenumbers of 469–536 and 3700 cm^{-1} are also related to the stretching vibration of the Al–O–Si and O–H groups in the clay.

In comparison, Bharadwaj *et al.* investigated the NaMMT treatment with phosphoric acid. They reported that the FTIR and XRD analysis of treated NaMMT showed no significant change compared to primary NaMMT. They also reported that the reason for increasing the clay surface was the production of silicon oxide, removing aluminum and amorphous silicon components, crick superficial porosity or interlayer spaces, and the formation of grooves and cavities at the surface[43]. According to Fig. 1(c), the FTIR analysis showed a similar result to Bharadwaj *et al.*, in which the FTIR analysis of treated NaMMT by nitric acid had not changed compared to the initial state. The interaction of nitric acid with Si–O and Al caused the closure of the pores and the distance between the sheets. However, the closure of the pores reduces the total surface area but increases the usable and available surface area for adsorption of DOX. Hence, it can be inferred that the studied adsorbents have a porous structure and numerous functional groups on their surface that have the potential to be used as adsorbents for the removal of DOX.

Adsorption kinetics

The contact time had an apparent effect on eliminating DOX. Fig. 2 shows the effect of contact time on removal efficiency. The experiments were conducted at ambient temperature to investigate the adsorption kinetics until the amount of drug adsorption on the adsorbents reached equilibrium. Overall means for each experiment, based on the average of the duplicates, are given. According to Fig. 2(a), it can be observed that the adsorption capacity of pure MWCNT increased rapidly during the first 10 min, and the adsorption equilibrium was attained after approximately 250 min. In the first 10 minutes, the active adsorption sites on MWCNT were gradually occupied, the adsorption rate decreased with increasing contact time until after 250 minutes, and there was no change in the concentration of the drug remaining in the solution. Furthermore, the adsorption of DOX on the treated MWCNT reached equilibrium in 40 min, compared to that of pure MWCNT, which was 250 min, indicating the significant effect of nitric acid treatment of DOX on the adsorption capacity, while equilibrium time reduced

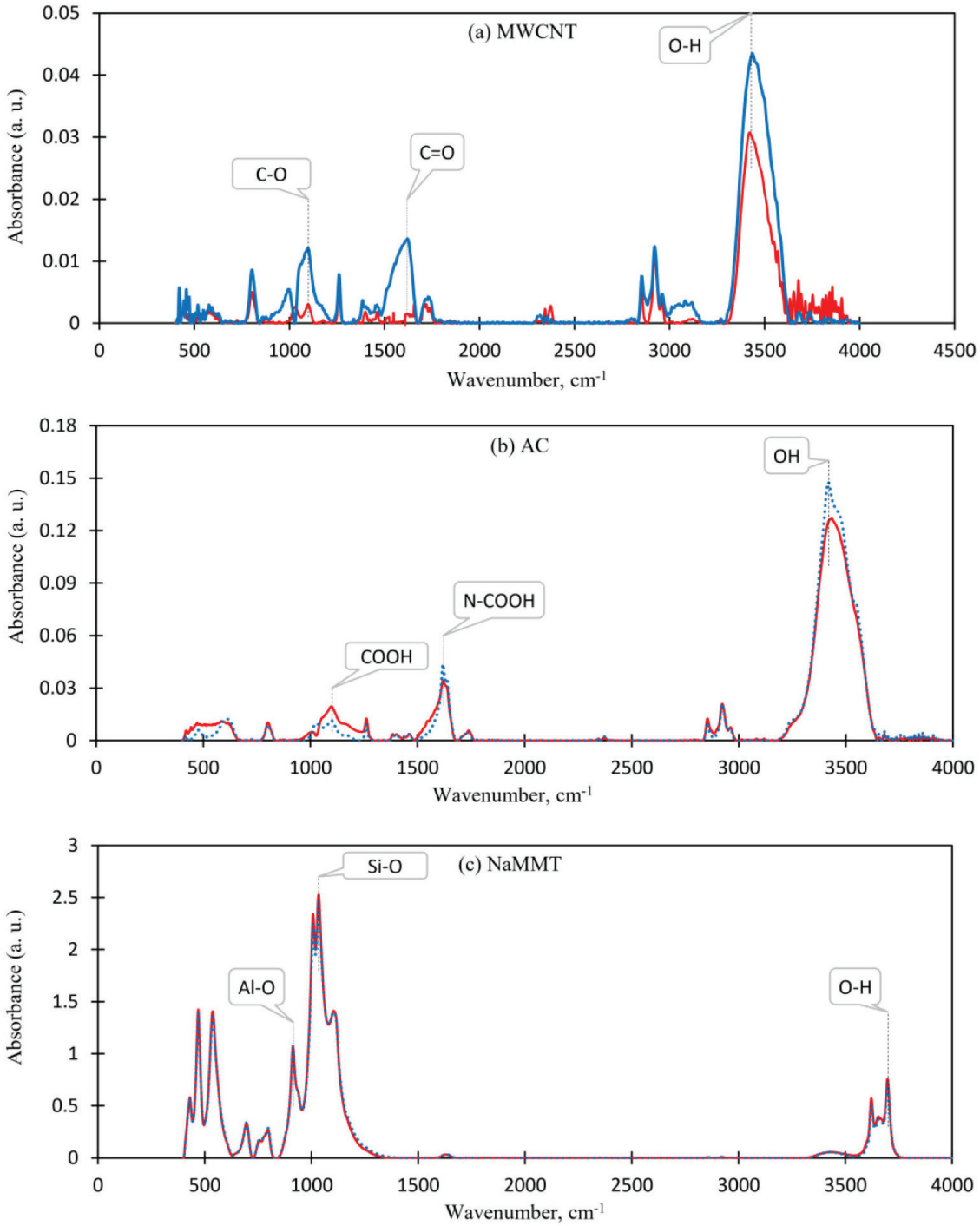

Fig. 1 – *FTIR spectra of (a) MWCNT, (b) AC, and (c) NaMMT. Solid lines and dashed lines represent before and after acid treatment, respectively.*

by 84 %. In this context, Weng *et al.*[44] reported that Fe_3O_4 nanoparticles for DOX adsorption required 24 h to reach equilibrium, meaning that the result obtained in this study is encouraging. As shown in Fig. 2(b), pure AC's adsorption capacity increased rapidly during the first 60 min, and the adsorption equilibrium was achieved after 150 min. By comparing the adsorption of DOX onto AC before and after acid treatment, it is evident that the changes are negligible. In fact, the treatment of AC with nitric acid was not effective. According to Fig. 2(c), almost 50 % of the total adsorption occurred in the first 25 min, and then the adsorption rate decreased gradually until it reached equilibrium in 180 min. The equilibrium adsorption time of DOX on the treated NaMMT was obtained at 60 min. In comparison, this period in the untreated NaMMT was 180 min, which indicated the positive effect of nitric acid treatment and reduced the equilibrium time by 67 %.

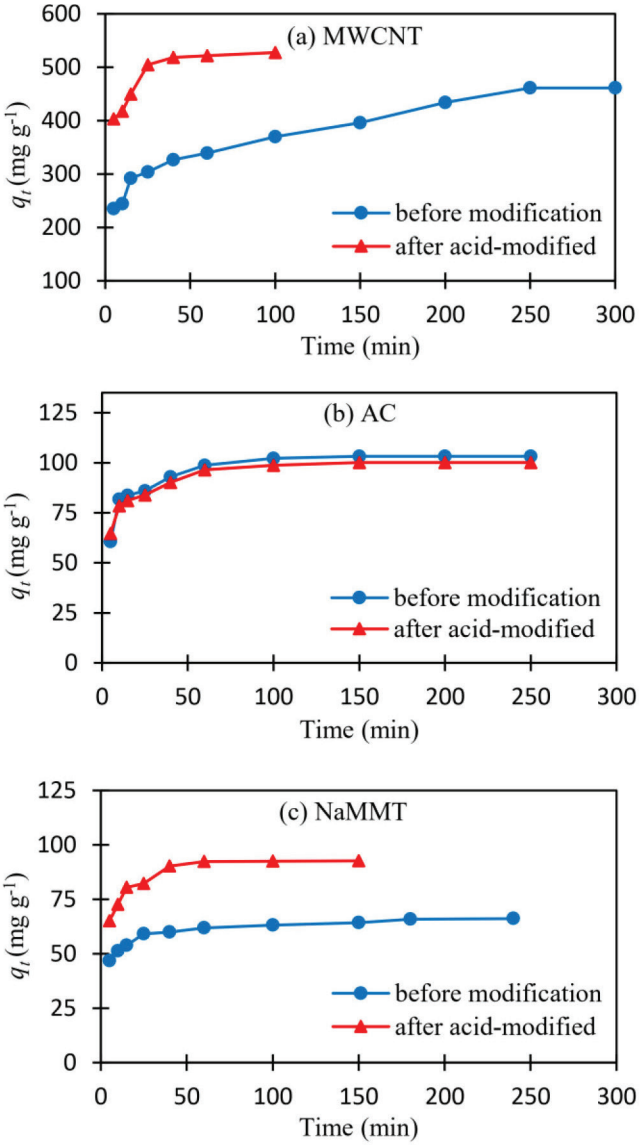

Fig. 2 – *Kinetic curves for adsorption of DOX on pure and treated: (a) MWCNT, (b) AC, and (c) NaMMT. DOX initial concentration was 50 mg L^{-1}; MWCNT, AC, and NaMMT dosages were 1, 5, and 10 mg, respectively, at pH = 6.5*

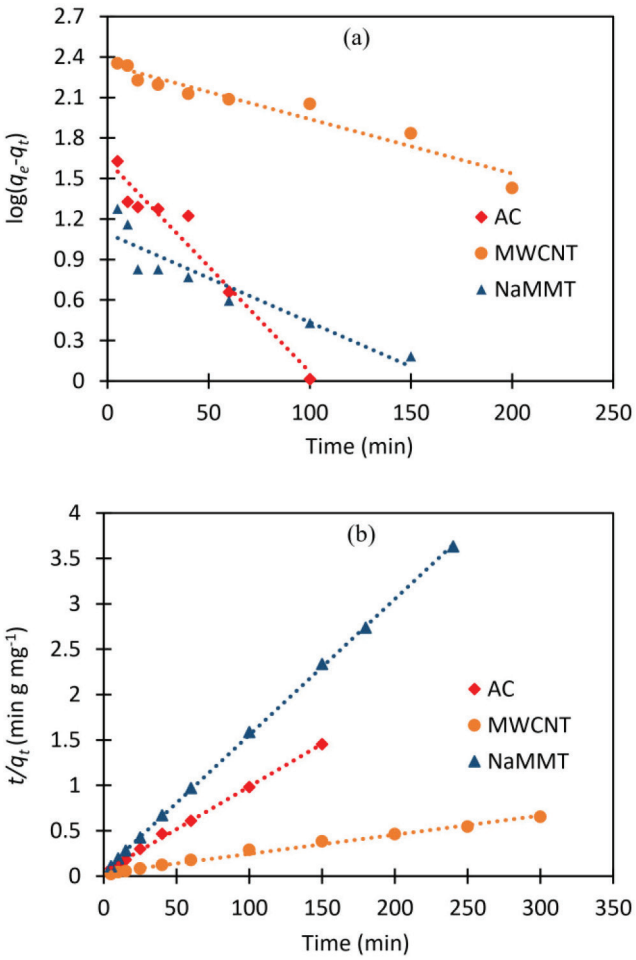

Fig. 3 – *Plot of the linearized adsorption kinetic models of DOX adsorption onto MWCNT, AC, and NaMMT at an initial concentration of 50 mg L^{-1} at pH= 6.5: (a) pseudo-first-order, and (b) pseudo-second-order*

Fig. 3 shows the alignment between experimental data and both the pseudo-first-order and pseudo-second-order kinetic models. Additionally, Table 1 presents the parameters of the pseudo-first-order and pseudo-second-order kinetic models for the adsorption of DOX on the three adsorbents. The linear correlation coefficient R^2 values provided in Table 1, derived from Fig. 3, indicate that the experimental data conform to a pseudo-second-order kinetic model for all three adsorbents.

As a result, it can be concluded that in the adsorption process of DOX from aqueous solutions on these three adsorbents, the chemical interaction between the functional groups of DOX and the adsorbent surface played an important role. In other words, the adsorption of DOX on the surface of MWCNT was primarily due to chemisorption. Therefore, the rate constants obtained from the

Table 1 – *Parameters of the kinetic models for the adsorption of DOX onto the studied adsorbents*

Adsorbent	Pseudo-first-order			Pseudo-second-order		
	q_{e1} (mg g^{-1})	k_1 (s^{-1})	R^2	q_{e2} (mg g^{-1})	k_2 (g s mg^{-1})	R^2
AC	42.63	0.0156	0.94	106.38	0.0019	0.99
MWCNT	220.34	0.004	0.93	476.19	0.0012	0.99
NaMMT	12.36	0.0066	0.86	66.67	0.0039	0.99

pseudo-second-order kinetic model follow the ascending order: MWCNTs < AC < NaMMT, indicating that NaMMT possesses more superficial functional groups available for interactions with DOX.

Adsorption isotherms

The effect of increasing the initial concentration of DOX on the removal efficiency of MWCNT, AC, and NaMMT is presented in Fig. 4.

As shown in Fig. 4, increasing the initial concentration of DOX from 25 to 50 mg L^{-1} resulted in a decrease in drug removal efficiency from 79 to 46 % for MWCNT, 64 to 50 % for AC, and 95 to 65 % for NaMMT. Essentially, as the initial concentration of the drug increased, the adsorption rate of the drug molecules decreased, leading to a decline in removal efficiency. This suggests that, once a sufficient amount of DOX occupies all adsorbent active sites, no further adsorption is possible. The adsorption performance and capacity of the adsorbent in removing DOX from an aqueous solution were assessed using isotherm models[45]. Fig. 5 shows the fitting of the experimental data with the Langmuir and Freundlich isotherms, both before and after the acid treatment of the three adsorbents. Additionally, Table 2 presents the Langmuir and Freundlich isotherm constants for both pure and treated adsorbents. The R^2 values indicated that the Langmuir model fitted well with the experimental data for all three adsorbents.

Table 3 reveals that the maximum adsorption capacities of DOX were found to be 500, 128.2, and 61.72 mg g^{-1} on MWCNTs, AC, and NaMMT, respectively, before acid treatment. It can be concluded that while the adsorption rate on NaMMT was higher, MWCNT exhibited a stronger tendency to adsorb DOX compared to the other two adsorbents. However, MWCNT with an adsorption capacity of 588.23 mg g^{-1}, and NaMMT with 105.26 mg g^{-1}, exhibited higher adsorption capacity after acid treatment. In other words, acid treatment increased the

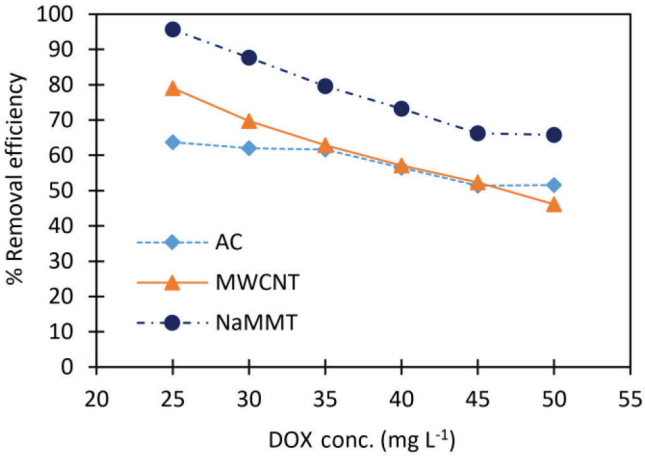

Fig. 4 – *Effect of initial concentration of DOX on the removal efficiency of MWCNT, AC, and NaMMT*

adsorption capacity of MWCNT and NaMMT by 15 % and 41 %, respectively. However, as mentioned previously, the maximum adsorption capacity of AC remained unchanged after acid treatment. A significant finding is the notably higher adsorption capacity of treated MWCNT and AC compared to their pure counterparts. This increase in capacity is likely due to their strong interactions with DOX molecules via H-bonding and increased access to adsorption sites, as indicated in the FTIR analysis section.

Moreover, the maximum adsorption capacity of MWCNT in this study (588.2 mg g^{-1}) greatly surpasses the 185.2 mg g^{-1} reported in the literature[37]. Hence, the adsorption performance and maximum capacity of DOX on different adsorbent materials depend on the availability of functional groups and the accessibility of the surface area. Despite their high adsorption capacities, these adsorbents are relatively expensive. Therefore, choosing an adsorbent with a high adsorption capacity such as carbon nanotubes, even at a relatively high price, may be justifiable.

Table 2 – *Parameters of the adsorption isotherms before and after acid treatment of adsorbent at ambient temperature*

Adsorbent	Langmuir			Freundlich		
	q_m (mg g^{-1})	b_l (L mg^{-1})	R^2	k_F	$\frac{1}{n_F}$	R^2
AC	128.2	0.121	0.985	28.88	0.382	0.92
MWCNT	500	0.61	0.999	324.86	0.118	0.990
NaMMT	61.72	1.86	0.999	47.4	0.082	0.992
Acid-treated AC	128.2	0.121	0.985	–	–	–
Acid-treated MWCNT	588.23	0.0137	0.947	152.9	0.32	0.873
Acid-treated NaMMT	105.26	0.0238	0.978	35.98	0.4	0.883

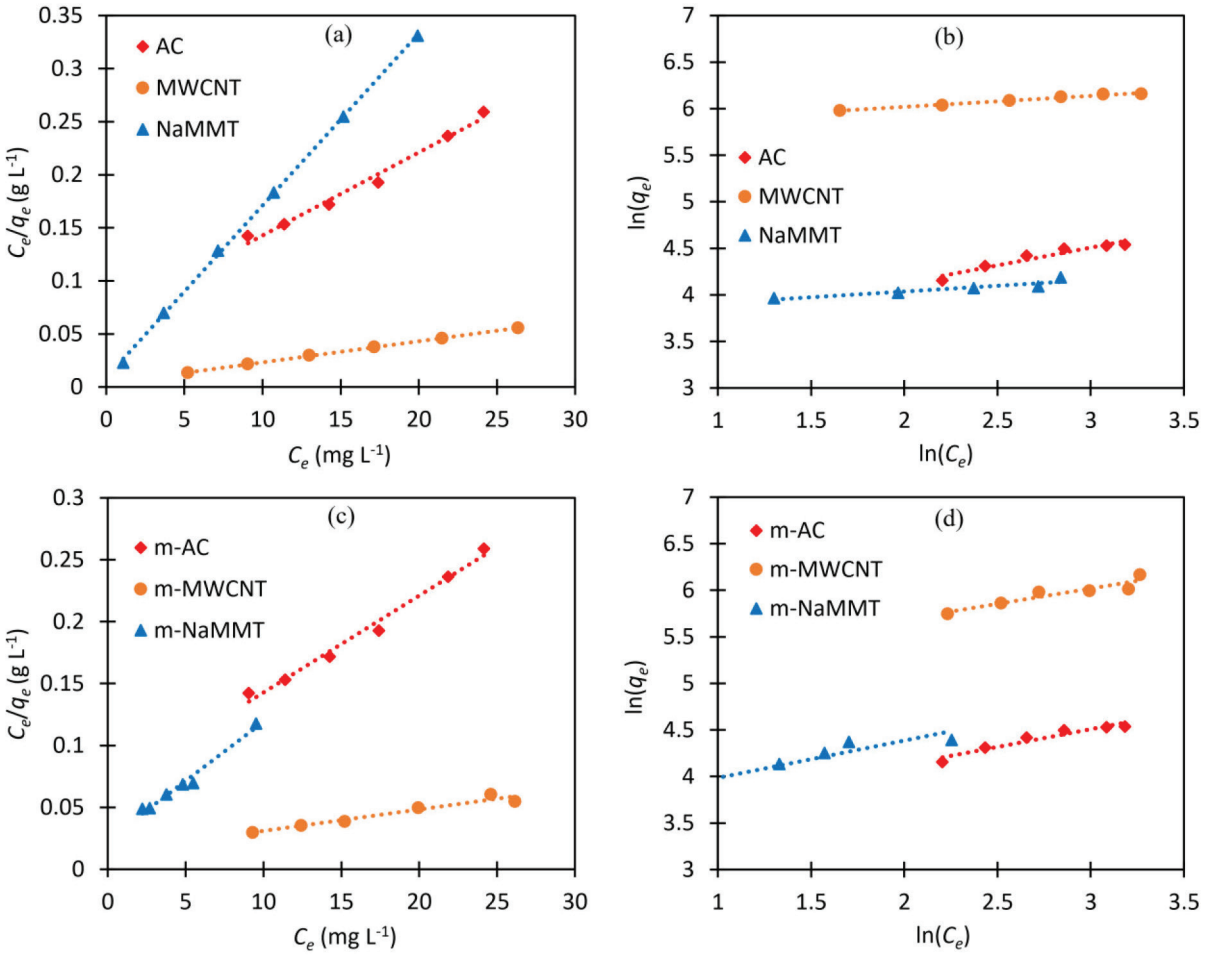

Fig. 5 – *Adsorption isotherms: (a) Langmuir, and (b) Freundlich for untreated adsorbents; (c) Langmuir, and (d) Freundlich for acid-modified adsorbents*

Effect of pH

Considering that pH significantly influences the surface charge of adsorbents and the degree of ionization, it emerges as a critical parameter in determining adsorption properties. To investigate the effect of pH value on the adsorption of DOX onto MWCNTs and AC, the equilibrium concentration was determined by varying the pH value from 5 to 10. As illustrated in Fig. 6, the amount of adsorbed DOX increased with rising pH within the studied range. For MWCNT, the adsorbed amount of DOX changed sharply with increasing pH, whereas for AC, no considerable change was observed at pH higher than eight. This observation can be attributed to the much higher electron-donating force at high pH values, where the –OH functional group, which is a solid electron-donation group, undergoes reduction to –O upon detachment of the electron, and the π-π interactions between the DOX and the MWCNT are strengthened[46], resulting in increased adsorption. The adsorption of DOX on CNT and AC is influenced by pH, which affects the protonation of the $–NH_2$ group on DOX and the surface charge of

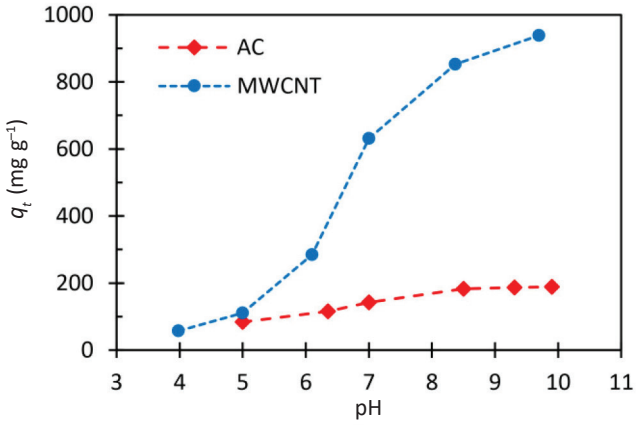

Fig. 6 – *Effect of solution pH on the adsorption of DOX onto MWNT and AC with an initial concentration of 50 mg L^{-1}*

the adsorbents. At low pH, the $–NH_2$ group is more protonated, weakening the hydrophobic interaction between CNT and DOX. Conversely, at high pH, the surfaces of CNT and AC become more negatively charged, increasing the attraction between

Table 3 – *Comparison of the adsorption capacity of doxorubicin on different adsorbents*

Adsorbent	Adsorption percentage	Temperature (K)	Equilibrium time	pH	Maximum adsorption capacity (mg g^{-1})	Ref.
Graphene oxide	~100 %	288–310	20 min	8.5	1428.6	[38]
Activated sludge	> 90 %	298	24 h	7.5	---	[47]
Fe_3O_4 nanoparticles	80.2 %	303	35 h	7–8	106.4	[44]
Carbon nanotubes	75 %	298	1.5 h	7.4	185.2	[37]
Magnetic copper Phosphate nanoflowers	95 %	298	1 h	8.2	1000	[3]
Functionalized Fe_3O_4@SiO_2 magnetic nanoparticles	92 %	303	80 h	7.4	72	[48]
Functionalized multi-walled carbon nanotubes (MWNTs)	95 %	298	35 min	7	41.6	[49]
MCM-41-type silica	–	293	24 h	7	153.3	[50]
Acid-treated activated carbon	63 %	298	4 h	8	128.2	This work
Acid-treated Na-montmorillonite	96 %	298	2.5 h	7	105.3	This work
Acid-treated Multi-walled carbon nanotubes	79 %	298	1.6 h	10	588.2	This work

them and DOX. The optimal pH for adsorption was 10 for CNT and 8 for AC. Regarding the effect of pH on the adsorption of DOX onto NaMMT, the results exhibited no clear trend, while the adsorption rate fluctuated as pH changed. Given that the average pH of hospital wastewater is reported to be 7.5 in different literature, aiming at removing DOX from this type of wastewater, the application of AC is more suitable in terms of pH.

For better understanding, Table 3 summarizes the performance of several adsorbents in terms of maximum adsorption capacity and operating conditions, including equilibrium time, optimum pH, and adsorption percentage, as investigated in both literature and this study for DOX removal.

Conclusion

In this study, the adsorption capacities of doxorubicin on three acid-treated adsorbents — MWCNTs, AC, and NaMMT— were determined to be 588, 128.2, and 105.3 mg g^{-1}, respectively. The results indicated that acid treatment increased the capacity of MWCNTs by 15 % and NaMMT by 41 %, while no effect was observed on AC. Equilibrium and kinetic studies revealed that the Langmuir isotherm and the pseudo-second-order kinetic models provided the best fit with experimental data for all three adsorbents. Furthermore, the investigation revealed that increasing the solution pH enhanced the adsorption capacity. The sequence of DOX adsorption capacity was as follows: MWCNT > AC > NaMMT. Hence, the removal of DOX from hospital wastewater using a multi-walled carbon nanotube can be effective. MWCNT exhibited superior performance in terms of adsorption capacity, adsorption rate, and appropriate functionalization through acid treatment.

Symbols used

b – Langmuir adsorption constant, mg^{-1}
C_0 – initial concentration, mg L^{-1}
C_e – equilibrium concentration, mg L^{-1}
k_1 – rate constant of pseudo-first-order model, min^{-1}
k_2 – rate constant of pseudo-second-order model, g mg^{-1} min^{-1}
k_F – Freundlich constant, (mg g^{-1})(L mg^{-1})$^{1/n}$
n – Freundlich power constant, –
q_e – amount of doxorubicin at equilibrium time, mg g^{-1}
q_m – maximum adsorption capacity, mg g^{-1}
q_t – amount of adsorbed adsorbate at time t, mg g^{-1}
R^2 – coefficient of determination, –
t – contact time, min

References

1. *Bray, F., Ferlay, J., Soerjomataram, I., Siegel, R. L., Torre, L. A., Jemal, A.*, Global cancer statistics 2018: GLOBOCAN estimates of incidence and mortality worldwide for 36 cancers in 185 countries, CA Cancer J. Clin. **68(6)** (2018) 394.
doi: https://doi.org/10.3322/caac.21492

2. *Chopdey, P. K., Tekade, R. K., Mehra, N. K., Mody, N., Jain, N. K.,* Glycyrrhizin conjugated dendrimer and multi-walled carbon nanotubes for liver specific delivery of doxorubicin, J. Nanosci. Nanotechnol. **15(2)** (2015) 1088. doi: https://doi.org/10.1166/jnn.2015.9039
3. *Gao, L., He, Q., Xing, J., Ge, Z.*, Removal of doxorubicin by magnetic copper phosphate nanoflowers for individual urine source separation, Chemosphere **238** (2020) 124690. doi: https://doi.org/10.1016/j.chemosphere.2019.124690
4. *Towfighi, F., Rahbar Shahrouzi, J., Ghaffari, S., Tabatabaei-Nejad, S. A.*, The effect of graphene oxide and functionalized carbon nanotubes as additives on extraction of doxorubicin by polyethylene glycol 6000/sodium salts aqueous two-phase systems, Fluid Ph. Equilib. **500** (2019) 112250. doi: https://doi.org/10.1016/j.fluid.2019.112250
5. *Cheriyamundath, S., Vavilala, S. L.*, Nanotechnology-based wastewater treatment, Water Environ. J. **35(1)** (2020) 123. doi: https://doi.org/10.1111/wej.12610
6. *Besse, J. P., Latour, J. F., Garric, J.*, Anticancer drugs in surface waters, Environ. Int. **39(1)** (2012) 73. doi: https://doi.org/10.1016/j.envint.2011.10.002
7. *Ghodrati, A., Shahrouzi, J. R., Nemati, R., Pourjafari, N.*, Adsorptive removal of daunorubicin from water by graphene oxide, activated carbon, and multiwalled carbon nanotubes: Equilibrium and kinetic studies, Chem. Eng. Technol. **45(12)** (2022) 2203. doi: https://doi.org/10.1002/ceat.202200326
8. *Duman, O., Tunç, S., Bozoğlan, B. K., Polat, T. G.,* Removal of triphenylmethane and reactive azo dyes from aqueous solution by magnetic carbon nanotube-κ-carrageenan-Fe_3O_4 nanocomposite, J. Alloys Compd. **687** (2016) 370. doi: https://doi.org/10.1016/j.jallcom.2016.06.160
9. *Battak, N., Kamin, Z., Bahrun, M. H. V., Chiam, C. K., Peter, E., Bono, A.*, Removal of trace plant antibiotics from water systems by adsorption: A review, Chem. Eng. Technol. **45(10)** (2022) 1721. doi: https://doi.org/10.1002/ceat.202200032
10. *Ahmadijokani, F., Tajahmadi, S., Rezakazemi, M., Sehat, A. A., Molavi, H., Aminabhavi, T. M., Arjmand, M.*, Aluminum-based metal-organic frameworks for adsorptive removal of anti-cancer (methotrexate) drug from aqueous solutions, J. Environ. Manag. **277** (2021) 111448. doi: https://doi.org/10.1016/j.jenvman.2020.111448
11. *Khalil, A. M., Han, L., Maamoun, I., Tabish, T. A., Chen, Y., Eljamal, O., Zhang, S., Butler, D., Memon, F. A.*, Novel graphene-based foam composite as a highly reactive filter medium for the efficient removal of gemfibrozil from (waste)water, Adv. Sustain. Syst. **6(8)** (2022) 2200016. doi: https://doi.org/10.1002/adsu.202200016
12. *Duman, O., Tunç, S., Polat, T. G.,* Determination of adsorptive properties of expanded vermiculite for the removal of C. I. Basic Red 9 from aqueous solution: Kinetic, isotherm and thermodynamic studies, Appl. Clay Sci. **109** (2015) 22. doi: https://doi.org/10.1016/j.clay.2015.03.003
13. *Duman, O., Polat, T. G., Diker, C. Ö., Tunç, S.,* Agar/κ-carrageenan composite hydrogel adsorbent for the removal of Methylene Blue from water, Int. J. Biol. Macromol. **160** (2020) 823. doi: https://doi.org/10.1016/j.ijbiomac.2020.05.191
14. *Ahmad, S. Z. N., Wan Salleh, W. N., Ismail, A. F., Yusof, N., Mohd Yusop, M. Z., Aziz, F.*, Adsorptive removal of heavy metal ions using graphene-based nanomaterials: Toxicity, roles of functional groups and mechanisms, Chemosphere **248** (2020) 126008. doi: https://doi.org/10.1016/j.chemosphere.2020.126008
15. *Yu, F., Ma, J., Bi, D.,* Enhanced adsorptive removal of selected pharmaceutical antibiotics from aqueous solution by activated graphene, Environ. Sci. Pollut. Res. **22(6)** (2014) 4715. doi: https://doi.org/10.1007/s11356-014-3723-9
16. *Crini, G., Lichtfouse, E.,* Advantages and disadvantages of techniques used for wastewater treatment, Environ. Chem. Lett. **17(1)** (2018) 145. doi: https://doi.org/10.1007/s10311-018-0785-9
17. *Chandrasekaran, A., Patra, C., Narayanasamy, S., Subbiah, S.,* Adsorptive removal of ciprofloxacin and amoxicillin from single and binary aqueous systems using acid-activated carbon from *Prosopis juliflora*, Environ. Res. **188** (2020) 109825. doi: https://doi.org/10.1016/j.envres.2020.109825
18. *Rahbar Shahrouzi, J., Molaee, S., Ebadi, A., Towfighi, F., Bakhti, F.,* Investigation of effective parameters on adsorption of amoxicillin from aqueous medium onto activated carbon, Adv. Environ. Technol. **5(2)** (2019) 107. doi: https://doi.org/10.22104/AET.2020.3781.1187
19. *Bekci, Z., Seki, Y., Yurdakoc, M.,* Equilibrium studies for trimethoprim adsorption on montmorillonite KSF, J. Hazard. Mater. **133** (2006) 233. doi: https://doi.org/10.1016/j.jhazmat.2005.10.029
20. *Zha, S. X., Zhou, Y., Jin, X., Chen, Z.,* The removal of amoxicillin from wastewater using organobentonite, J. Environ. Manage. **129** (2013) 569. doi: https://doi.org/10.1016/j.jenvman.2013.08.032
21. *Sotelo, J. L., Ovejero, G., Rodríguez, A., Álvarez, S., García, J.,* Analysis and modeling of fixed bed column operations on flumequine removal onto activated carbon: pH influence and desorption studies, Chem. Eng. J. **228** (2013) 102. doi: https://doi.org/10.1016/j.cej.2013.04.088
22. *Bhatnagar, A., Hogland, W., Marques, M., Sillanpää, M.,* An overview of the modification methods of activated carbon for its water treatment applications, Chem. Eng. J. **219** (2013) 499. doi: https://doi.org/10.1016/j.cej.2012.12.038
23. *Li, Y. H., Ding, J., Luan, Z., Di, Z., Zhu, Y., Xu, C., Wu, D., Wei, B.*, Competitive adsorption of Pb^{2+}, Cu^{2+} and Cd^{2+} ions from aqueous solutions by multiwalled carbon nanotubes, Carbon **41(14)** (2003) 2787. doi: https://doi.org/10.1016/s0008-6223(03)00392-0
24. *Kathi, J., Rhee, K. Y.,* Surface modification of multi-walled carbon nanotubes using 3-aminopropyltriethoxysilane, J. Mater. Sci. **43(1)** (2007) 33. doi: https://doi.org/10.1007/s10853-007-2209-2
25. *Yu, J. G., Zhao, X. H., Yang, H., Chen, X. H., Yang, Q., Yu, L. Y., Jiang, J. H., Chen, X. Q.*, Aqueous adsorption and removal of organic contaminants by carbon nanotubes, Sci. Total Environ. **482** (2014) 241. doi: https://doi.org/10.1016/j.scitotenv.2014.02.129
26. *Li, R., Wu, R., Zhao, L., Zhao, L., Hu, Z., Guo, S., Pan, X., Zou, H.,* Folate and iron difunctionalized multiwall carbon nanotubes as dual-targeted drug nanocarrier to cancer cells, Carbon **49(5)** (2011) 1797. doi: https://doi.org/10.1016/j.carbon.2011.01.003
27. *Yang, W., Thordarson, P., Gooding, J. J., Ringer, S. P., Braet, F.,* Carbon nanotubes for biological and biomedical applications, Nanotechnology **18(41)** (2007) 412001. doi: https://doi.org/10.1088/0957-4484/18/41/412001
28. *Gojny, F. H., Nastalczyk, J., Roslaniec, Z., Schulte, K.*, Surface modified multi-walled carbon nanotubes in CNT/epoxy-composites, Chem. Phys. Lett. **370** (2003) 820. doi: https://doi.org/10.1016/s0009-2614(03)00187-8

29. *Thiebault, T.,* Raw and modified clays and clay minerals for the removal of pharmaceutical products from aqueous solutions: State of the art and future perspectives, Crit. Rev. Environ. Sci. Technol. **50(14)** (2019) 1451. doi: https://doi.org/10.1080/10643389.2019.1663065
30. *Putra, E. K., Pranowo, R., Sunarso, J., Indraswati, N., Ismadji, S.*, Performance of activated carbon and bentonite for adsorption of amoxicillin from wastewater: Mechanisms, isotherms and kinetics, Water Res. **43(9)** (2009) 2419. doi: https://doi.org/10.1016/j.watres.2009.02.039
31. *Jayrajsinh, S., Shankar, G., Agrawal, Y. K., Bakre, L.,* Montmorillonite nanoclay as a multifaceted drug-delivery carrier: A review, J. Drug Deliv. Sci. Technol. **39** (2017) 200. doi: https://doi.org/10.1016/j.jddst.2017.03.023
32. *Mashburn, C. D., Frinak, E. K., Tolbert, M. A.,* Heterogeneous uptake of nitric acid on Na-montmorillonite clay as a function of relative humidity, J. Geophys. Res. **111** (2006) D15. doi: https://doi.org/10.1029/2005jd006525
33. *Bhattacharyya, K. G., Gupta, S. S.,* Adsorption of a few heavy metals on natural and modified kaolinite and montmorillonite: A review, Adv. Colloid Interface Sci. **140(2)** (2008) 114. doi: https://doi.org/10.1016/j.cis.2007.12.008
34. *Hasanzade, Z., Raissi, H.,* Density functional theory calculations and molecular dynamics simulations of the adsorption of ellipticine anticancer drug on graphene oxide surface in aqueous medium as well as under controlled pH conditions, J. Mol. Liq. **255** (2018) 269. doi: https://doi.org/10.1016/j.molliq.2018.01.159
35. *Chen, Z., Pierre, D., He, H., Tan, S., Pham-Huy, C., Hong, H., Huang, J.*, Adsorption behavior of epirubicin hydrochloride on carboxylated carbon nanotubes, Int. J. Pharm. **405** (2011) 153. doi: https://doi.org/10.1016/j.ijpharm.2010.11.034
36. *Tońska, M., Dołżonek, J., Paszkiewicz, M., Wojsławski, J., Stepnowski, P., Białk-Bielińska, A.*, Preliminary evaluation of the application of carbon nanotubes as potential adsorbents for the elimination of selected anticancer drugs from water matrices, Chemosphere **201** (2018) 32. doi: https://doi.org/10.1016/j.chemosphere.2018.02.072
37. *Chudoba, D., Łudzik, K., Jażdżewska, M., Wołoszczuk, S.,* Kinetic and equilibrium studies of doxorubicin adsorption onto carbon nanotubes, Int. J. Mol. Sci. **21** (2020) 8230. doi: https://doi.org/10.3390/ijms21218230
38. *Wu, S., Zhao, X., Li, Y., Du, Q., Sun, J., Wang, Y., Wang, X., Xia, Y., Wang, Z., Xia, L.*, Adsorption properties of doxorubicin hydrochloride onto graphene oxide: Equilibrium, kinetic and thermodynamic studies, Materials **6(5)** (2013) 2026. doi: https://doi.org/10.3390/ma6052026
39. *Lucaci, A. R., Bulgariu, D., Popescu, M. C., Bulgariu, L.,* Adsorption of Cu(II) ions on adsorbent materials obtained from marine red algae *Callithamnion corymbosum* sp, Water **12(2)** (2020) 372. doi: https://doi.org/10.3390/w12020372
40. *Tunç, S., Duman, O.,* The effect of different molecular weight of poly(ethylene glycol) on the electrokinetic and rheological properties of Na-bentonite suspensions, Colloids Surf. A: Physicochem. Eng. Asp. **317** (2008) 93. doi: https://doi.org/10.1016/j.colsurfa.2007.09.039
41. *Pan, B., Xing, B.,* Adsorption mechanisms of organic chemicals on carbon nanotubes, Environ. Sci. Technol. **42(24)** (2008) 9005. doi: https://doi.org/10.1021/es801777n
42. *Bahrami, M., Amiri, M. J., Mahmoudi, M. R., Koochaki, S.,* Modeling caffeine adsorption by multi-walled carbon nanotubes using multiple polynomial regression with interaction effects, J. Water Health **15(4)** (2017) 526. doi: https://doi.org/10.2166/wh.2017.297
43. *Bharadwaj, S. K., Boruah, P. K., Gogoi, P. K.,* Phosphoric acid modified montmorillonite clay: A new heterogeneous catalyst for nitration of arenes, Catal. Commun. **57** (2014) 124. doi: https://doi.org/10.1016/j.catcom.2014.08.019
44. *Weng, X., Ma, L., Guo, M., Su, Y., Dharmarajan, R., Chen, Z.*, Removal of doxorubicin hydrochloride using Fe_3O_4 nanoparticles synthesized by euphorbia cochinchinensis extract, Chem. Eng. J. **353** (2018) 482. doi: https://doi.org/10.1016/j.cej.2018.07.162
45. *Tunç, S., Duman, O., Kancı, B.,* Rheological measurements of Na-bentonite and sepiolite particles in the presence of tetradecyltrimethylammonium bromide, sodium tetradecyl sulfonate and Brij 30 surfactants, Colloids Surf. A: Physicochem. Eng. Asp. **398** (2012) 37. doi: https://doi.org/10.1016/j.colsurfa.2012.02.006
46. *Chen, W., Duan, L., Wang, L., Zhu, D.,* Adsorption of hydroxyl- and amino-substituted aromatics to carbon nanotubes, Environ. Sci. Technol. **42(18)** (2008) 6862. doi: https://doi.org/10.1021/es8013612
47. *Mahnik, S., Lenz, K., Weissenbacher, N., Mader, R., Fuerhacker, M.,* Fate of 5-fluorouracil, doxorubicin, epirubicin, and daunorubicin in hospital wastewater and their elimination by activated sludge and treatment in a membrane-bio-reactor system, Chemosphere **66(1)** (2007) 30. doi: https://doi.org/10.1016/j.chemosphere.2006.05.051
48. *Cai, W., Guo, M., Weng, X., Zhang, W., Chen, Z.*, Adsorption of doxorubicin hydrochloride on glutaric anhydride functionalized Fe_3O_4@SiO_2 magnetic nanoparticles, Mater. Sci. Eng. C **98** (2019) 65. doi: https://doi.org/10.1016/j.msec.2018.12.145
49. *Farahani, B. V., Behbahani, G. R., Javadi, N.,* Functionalized multi walled carbon nanotubes as a carrier for doxorubicin: Drug adsorption study and statistical optimization of drug loading by factorial design methodology, J. Braz. Chem. Soc. **27(4)** (2016) 694. doi: https://doi.org/10.5935/0103-5053.20150318
50. *Roik, N. V., Belyakova, L. A., Dziazko, M. O.,* Adsorption of antitumor antibiotic doxorubicin on MCM-41-type silica surface, Adsorpt. Sci. Technol. **35(1-2)** (2017) 86. doi: https://doi.org/10.1177/0263617416669504